Environmental Science and Pollution Research (2019) 26:4337–4347
https://doi.org/10.1007/s11356-018-2555-4

ADVANCED OXIDATION TECHNOLOGIES: STATE-OF-THE-ART IN IBERO-AMERICAN COUNTRIES

Direct and indirect photolysis of the antibiotic enoxacin: kinetics of oxidation by reactive photo-induced species and simulations

Arlen Mabel Lastre-Acosta[1] · Bruna Barberato[1] · Marcela Prado Silva Parizi[2] · Antonio Carlos Silva Costa Teixeira[1]

Received: 31 January 2018 / Accepted: 13 June 2018 / Published online: 21 June 2018

Abstract

The purpose of this study was to investigate the aqueous phase photochemical behavior of enoxacin (ENO), an antibiotic selected as a model pollutant of emerging concern. The second-order reaction rate constants of ENO with hydroxyl radicals ($HO^{\bullet}$) and singlet oxygen ($^1O_2$) were determined at pH 3, 7, and 9. Also, the rate constants of the electron transfer reaction between ENO and triplet states of chromophoric dissolved organic matter (^{3}CDOM*) are reported for the first time, based on anthraquinone-2-sulfonate (AQ2S) as CDOM proxy. The sunlight-driven direct and indirect ENO degradation in the presence of dissolved organic matter (DOM) is also discussed. The results show that direct photolysis, which occurs more rapidly at higher pH, along with the reactions with $HO^{\bullet}$ and ^{3}AQ2S*, is the key pathway involved in ENO degradation. The ENO zwitterions, prevailing at pH 7, show $k_{ENO,\ HO^{\bullet}}$, $k_{ENO,1O2}$, and $k_{ENO,3AQ2S*}$ of $(14.0 \pm 0.8) \times 10^{10}$, $(3.9 \pm 0.2) \times 10^{6}$, and $(61.5 \pm 0.7) \times 10^{8}$ L mol^{-1} s^{-1}, respectively, whose differences at pH 3, 7, and 9 are due to ENO pH-dependent speciation and reactivity. These k values, along with the experimental ENO photolysis quantum yield, were used in mathematical simulations for predicting ENO persistence in sunlit natural waters. According to the simulations, dissolved organic matter and water depth are expected to have the highest impacts on ENO half-life, varying from a few hours to days in summertime, depending on the concentrations of relevant waterborne species (organic matter, NO_3^-, NO_2^-, HCO_3^-).

Keywords Enoxacin · Environmental photochemical fate · Reactive photo-induced species · Dissolved organic matter · Mathematical modeling · Direct and indirect photodegradation · Antibiotics

Introduction

Fluoroquinolone antibiotics (FQs) are an important class of drugs that are not effectively removed in wastewater treatment plants (Ge et al. 2015). As an example, high fluoroquinolone concentrations have been reported in the effluent from a drug manufacturing facility located in Patancheru, India (Larsson et al. 2007). In fact, six of the 11 most abundant pharmaceuticals detected at this site were fluoroquinolones (ciprofloxacin, enrofloxacin, norfloxacin, lomefloxacin, enoxacin, and ofloxacin), some of them present at concentrations of milligram per liter (Larsson et al. 2007). In turn, extraordinarily high concentrations of fluoroquinolones like ciprofloxacin (6.5 mg L^{-1}), cetirizine (1.2 mg L^{-1}), norfloxacin (0.52 mg L^{-1}), and enoxacin (0.16 mg L^{-1}) associated with pharmaceutical production and formulation have been detected in the same region (Fick et al. 2009).

Responsible editor: Suresh Pillai

Electronic supplementary material The online version of this article (https://doi.org/10.1007/s11356-018-2555-4) contains supplementary material, which is available to authorized users.

✉ Arlen Mabel Lastre-Acosta
arlenlastre@gmail.com

✉ Marcela Prado Silva Parizi
marcela@rosana.unesp.br

[1] Research Group in Advanced Oxidation Processes (AdOx), Chemical Systems Engineering Center, Department of Chemical Engineering, University of São Paulo, Av. Prof. Luciano Gualberto, tr. 3, São Paulo, SP 380, Brazil

[2] Department of Energy Engineering, São Paulo State University (UNESP), Av. Barrageiros, Rosana, SP 1881, Brazil

Enoxacin (1-ethyl-6-fluoro-1,4-dihydro-4-oxo-7-(1-piperazinyl)-1,8-naphthyridine-3-carboxylic acid, hereinafter referred as ENO) is one of the third-generation fluoroquinolones, containing in its chemical structure a naphthyridine ring in place of the quinoline ring (Sortino et al. 1998). Owing to its good absorption and low frequency of adverse effects (Liu et al. 2010), ENO is used in the treatment of certain infections of the urinary, respiratory, gastrointestinal tracts, and skin (Tong and Xiang 2007), primarily inhibiting bacterial DNA-gyrase in cells (Tong and Xiang 2007).

In general, FQs show resistance to hydrolysis and biodegradation, but their susceptibility to UV-visible light has been demonstrated (Ge et al. 2015). In fact, two classes of photochemical mechanisms, both direct and indirect, can represent major FQ removal pathways in surface waters (Ge et al. 2015). Direct photodegradation can occur by sunlight absorption, and indirect photolysis involves reactions with reactive photo-induced species (RPS), namely singlet oxygen ($^1O_2$), hydroxyl radicals ($HO^\bullet$), the triplet excited state of chromophoric dissolved organic matter (^{3}CDOM*) formed in natural waters (Perisa et al. 2013) following light absorption by different species (nitrate, nitrite, dissolved organic matter, iron complexes, etc.). It is worth observing that the kinetics of enoxacin photochemical degradation is directly related to the pH-dependent speciation of this compound, which exhibits two pKa values (6.0 and 8.5) (Gao et al. 2011). Therefore, the zwitterionic form of enoxacin is the prevalent species in environmental waters, with pH values typically falling in the range 6–9.

FQs can also undergo self-sensitized photo-oxidation via $HO^\bullet$ radicals and $^1O_2$ (Ge et al. 2015). According to the generally accepted mechanism, FQ photoexcitation generates a triplet excited state, ^{3}FQ* (reactions 1 and 2), that gives photoproducts (reaction 3) or reacts with molecular oxygen, leading to the formation of oxidants such as singlet oxygen ($^1O_2$) (reaction 4) or the superoxide radical anion, along with the FQ radical cation (reaction 5) (Albini and Monti 2003; Porras et al. 2016). Moreover, according to Ji et al. (2013), H_2O and dissolved oxygen may act as ^{3}FQs*quenchers, giving hydroxyl radicals.

$$FQ + h\nu \rightarrow {}^1FQ^* \quad (1)$$

$${}^1FQ^* \rightarrow {}^3FQ^* \quad (2)$$

$${}^3FQ^* \rightarrow photoproducts \quad (3)$$

$${}^3FQ^* + O_2 \rightarrow FQ + {}^1O_2 \quad (4)$$

$${}^3FQ^* + O_2 \rightarrow FQ^{\bullet+} + O_2^{\bullet-} \quad (5)$$

In any case, the knowledge of the bimolecular reaction rate constants $k_{ENO,HO^\bullet}$, $k_{ENO,1O2}$, and $k_{ENO,3CDOM*}$ allows the evaluation of the relative contribution of every RPS ($HO^\bullet$, $^1O_2$, and ^{3}CDOM*) towards ENO photodegradation in natural and engineered water systems (Escalada et al. 2014). However, information regarding these kinetic rate constants with different pH-dependent forms of ENO is still largely unknown.

In this context, the aim of this study was to understand the photochemical behavior of enoxacin (ENO) in aqueous systems. For this purpose, the reaction rate constants of ENO with $HO^\bullet$ and $^1O_2$ at pH 3, 7, and 9 were determined. In addition, to the best of our knowledge, the second-order reaction rate constants between ENO and ^{3}CDOM* (using anthraquinone-2-sulfonate (AQ2S) as CDOM proxy) at these pH are discussed for the first time. This kinetic constant ($k_{ENO,3AQ2S*}$), along with $k_{ENO,\ HO\cdot}$, and $k_{ENO,1O2}$ values, and information on ENO photolysis quantum yield are used in mathematical simulations for predicting ENO half-life times in sunlit waters with different physicochemical characteristics. Additionally, the sunlight-driven direct and indirect ENO degradation in the presence of dissolved organic matter (DOM) is discussed.

Materials and methods

Reagents

All the solutions were prepared by dissolving enoxacin (ENO) > 98% ($C_{15}H_{17}FN_4O_3 \cdot 1.5H_2O$) (Sigma-Aldrich) in ultrapure water (Milli-Q). Methylene blue, acquired from Synth, and furfuryl alcohol (FFA), provided by Sigma-Aldrich, were used as the $^1O_2$ source and the reference compound, respectively. Additionally, H_2O_2 (the $HO^\bullet$ source) and para-chlorobenzoic acid (*p*CBA, the reference compound) were obtained from Synth and Sigma-Aldrich, respectively. Anthraquinone-2-sulfonate (AQ2S), used as proxy for CDOM and 2,4,6-trimethylphenol (TMP), used as the reference compound, were obtained from Sigma-Aldrich.

Suwannee River Natural Organic Matter (SRNOM) was acquired from the International Humic Substances Society (Catalog No. 1R101N). Aldrich humic acid sodium salt (AHA) was obtained from Sigma-Aldrich. The urban-waste bio-organic substance (UW-BOS), identified by the acronym CVT230 (Arques and Bianco Prevot 2015), was obtained from the process lines of ACEA Pinerolese waste treatment plant in Pinerolo (Italy) and has been isolated from home gardening and park trimming residue piles aerated for 230 days (Montoneri et al. 2011). Stock solutions of these organic matters were prepared in a phosphate buffer solution (pH 7.1).

To prepare the mobile phase for the HPLC system, methanol (HPLC quality) and acetic acid (80% *v*/*v*) were purchased from Panreac and Scharlau, respectively.

Photodegradation experiments

ENO photodegradation experiments were performed using a solar simulator (Newport, 91160) equipped with a 450-W xenon lamp and an AM 1.5 global filter, providing 68 W m^{-2} in the wavelength range 290–800 nm. The samples were contained in 2-mL Pyrex vials with no headspace and exposed to light while kept in a water bath to maintain an average temperature of 25 °C. The radiation source was positioned over the vials at a distance of 15 cm; the irradiated pathlength inside the vials was 10 mm.

The bimolecular reaction rate constants at pH 3, 7, and 9 were determined to understand the reactivity of each protonation state of ENO towards RPS ($^1O_2$, $HO^\bullet$, $^3CDOM^*$). Solution pH was adjusted to the initial desired value but not corrected over reaction time.

The simulated sunlight-driven direct and indirect ENO degradation (through $HO^\bullet$, $^1O_2$), at $[ENO]_0 = 15.6$–156.1 μmol L^{-1} (5–50 mg L^{-1}), and in the presence of isolated natural organic matter (NOM) was investigated following the methodology detailed by Silva et al. (2015). The initial ENO concentration range was selected to allow HPLC quantification without using pre-concentration steps, thus preventing the introduction of variability in the experimental data.

In order to study the reactivity between ENO and the triplet state of organic matter, AQ2S was used as a proxy for CDOM, based on the fact that quinones are very common CDOM components and also for the reason that AQ2S irradiation does not yield interfering species such as $^1O_2$ and $HO^\bullet$ (Marchetti et al. 2013). In this study, the optimized initial AQ2S concentration was 30.5 μmol L^{-1}, low enough to prevent side reactions between the excited and ground states of AQ2S, which would occur at higher concentrations (≥ 0.1 mmol L^{-1}) (Bedini et al. 2012).

Analytical methods

An HPLC system (Shimadzu, LC20 model) equipped with a UV/Vis diode array detector (SPD20A model) and a RP18 column (Super Sphere 100 model, 250 mm × 4.6 mm; 5 μm) was used to follow ENO, *p*CBA, FFA, and TMP concentration-time profiles. The following conditions were used: ENO (270 nm, aqueous acetic acid 1% (*v*/*v*) (A) + acetonitrile (B), gradient elution: 0–2 min, 17% B; 2–3 min, 29% B; 3–7 min, 29% B; 7–8 min, 17% B; 8–14 min, 17% B); *p*CBA (234 nm, 50% aqueous acetic acid 1% (*v*/*v*) + 50% methanol, isocratic); FFA (219 nm, 70% aqueous acetic acid 1% (*v*/*v*) + 30% methanol, isocratic); TMP (220 nm, 50% aqueous acetic acid 1% (*v*/*v*) + 50% acetonitrile, isocratic). In all cases, the temperature, injected volume, and mobile phase flow rate were 40 °C, 100 μL, and 1 mL min^{-1}, respectively.

Kinetic study: hydroxyl radical, singlet oxygen, and triplet excited states of chromophoric dissolved organic matter

The second-order reaction rate constants between ENO and RPS ($k_{ENO,HO\cdot}$, $k_{ENO,1O2}$, and $k_{ENO,3AQ2S*}$) were determined using the competition kinetics method [4], according to Eq. (1).

$$k_{ENO,RPS} = \frac{\left(k_{ENO(obs)} - k_{ENO(direct\ phot)}\right)}{\left(k_{ref\ (obs)} - k_{ref\ (direct\ phot)}\right)} \times k_{ref,RPS} \quad (1)$$

where $k_{ENO,\ RPS}$ is the second-order rate constant of the reaction between ENO and RPS ($HO^\bullet$, $^1O_2$, and $^3AQ2S*$); $k_{ENO(obs)}$ is the measured pseudo first-order specific photolysis rate of ENO; $k_{ENO(direct\ phot)}$ and $k_{ref(direct\ phot)}$ are the measured photolysis rate constants of ENO and reference compound, respectively; $k_{ref\ (obs)}$ is the measured pseudo first-order specific photolysis rate of the reference compound (FFA, *p*CBA, and TMP); $k_{ref,\ ROS}$ is the second-order rate constant of the reaction between each reference compound and RPS: $k_{FFA,1O2} = 1.2 \times 10^8$ L mol^{-1} s^{-1} (Mostafa and Rosario-Ortiz 2013), $k_{pCBA,HO\cdot} = 5 \times 10^9$ L mol^{-1} s^{-1} (Elovitz and von Gunten 1999), and $k_{TMP,3CDOM*} = 3 \times 10^9$ L mol^{-1} s^{-1} (al Housari et al. 2010).

The second-order kinetic rate constant of ENO with $HO^\bullet$ ($k_{ENO,HO\cdot}$) was determined using H_2O_2 as the RPS source and *p*CBA as the reference compound (Silva et al. 2015); the concentrations used were 63.9 μmol L^{-1} (*p*CBA) and 50 mmol L^{-1} (H_2O_2). For $k_{ENO,1O2}$ determination, methylene blue (31.3 μmol L^{-1}) and furfuryl alcohol (40.8 μmol L^{-1}) were used as the $^1O_2$ source and the reference compound, respectively (Silva et al. 2015); methanol was added (0.1 mol L^{-1}) to quench $HO^\bullet$ radicals. Finally, in the case of $k_{ENO,3AQ2S*}$, AQ2S and TMP concentrations were 30.5 and 36.7 μmol L^{-1}, respectively. These concentrations were optimized for the experiments with ENO based on previous works (Marchetti et al. 2013; Silva et al. 2015).

Photochemical simulations

The mathematical simulations of ENO sunlight-driven environmental degradation were carried out with the APEX model (Aqueous Photochemistry of Environmentally Occurring Xenobiotics) (Bodrato and Vione 2014). This model is used to calculate half-life times based on the chemical composition of water and irradiation depth, knowing the pollutant photolysis quantum yield under sunlight and the experimental second-order reaction rate constants with $HO^\bullet$, $^1O_2$, and $^3CDOM*$. The APEX model has been validated by comparison with field data of pharmaceutical compound phototransformation kinetics in surface freshwaters (De Laurentiis et al. 2014; Vione et al. 2011). More details about the model

equations can be found at http://chimica.campusnet.unito.it/do/didattica.pl/ Show?_id=4pyh. The standardized time unit in the model is a summer sunny day corresponding to 10 h of continuous irradiation at 22 W m^2 irradiance.

The following range of values, based on data reported for Brazilian surface waters (Silva et al. 2015), were selected for the independent variables used in simulations: dissolved organic carbon (DOC) = 0.5–10 mg L^{-1} (corresponding to DOM); water depth: 0.5–5 m; nitrate: $[NO_3^-] = 1.0–1.0 \times 10^2$ μmol L^{-1}; nitrite: $[NO_2^-] = 5.0 \times 10^{-2}–15$ μmol L^{-1}; $[HCO_3^-] = 2.0 \times 10^2–2.0 \times 10^3$ μmol L^{-1}; pH 7.

Results and discussion

ENO photolysis: effect of initial concentration

Figure 1 shows the results obtained for the solar-driven ENO photolytic degradation in Milli-Q water at pH 7. ENO decay was affected by its initial concentration, with specific photolysis rates of $(9.5 \pm 0.16) \times 10^{-2}$ ($R^2 = 0.974$), $(9.0 \pm 0.63) \times 10^{-2}$ ($R^2 = 0.973$), $(6.1 \pm 0.27) \times 10^{-2}$ ($R^2 = 0.979$), $(5.3 \pm 0.32) \times 10^{-2}$ ($R^2 = 0.992$), and $(3.1 \pm 0.07) \times 10^{-2}$ ($R^2 = 0.991$) min^{-1} for initial ENO concentrations of 15.6, 31.2, 62.4, 93.7, and 156.1 μmol L^{-1}, respectively. As shown in the inset of Fig. 1, an increase in initial ENO concentration resulted in a proportional decrease in the corresponding specific ENO photolysis rates.

Li et al. (2014) investigated the effect of the initial concentration on the photodegradation kinetics and hydroxyl radical-driven oxidation of thiamphenicol and florfenicol. They found that these antibiotics under direct photolysis and self-sensitized photo-oxidation were rapidly removed and the slopes of the corresponding k vs. C_0 plots were negative. These authors associate such behavior to the attenuation of light transmission for higher initial concentrations.

This behavior has been also associated with self-sensitization via reactive oxygen species. Following this reasoning, direct photolysis (which depends on the quantum yield and on solute concentration according to the Beer-Lambert Law) and second-order reactions with reactive species (for instance, hydroxyl radicals) are simultaneous and competitive degradation pathways during solute irradiation, whose decay is usually described in the literature by simple pseudo first-order models. In fact, according to Li et al. (2014) and Ge et al. (2015), the triplet excited FQs are quenched by water and dissolved oxygen molecules, giving $HO^•$ radicals, therefore suppressing FQ direct photolysis. As a consequence, the self-sensitized photooxidation would play a major role with increasing initial concentration, with direct photolysis contributing less to solute degradation. As pointed out by Ge et al. (2015), this effect has been also reported for other self-sensitized molecules (Gangwang et al. 2012; Li et al. 2014).

In addition, it should be remembered that pollutant concentration-dependent quantum yields for the UV photolysis of some organic compounds have been also discussed in the literature (e.g., Hessler et al. 1993). All these factors taken together would explain the observed behavior of pseudo first-order k values with $[ENO]_0$.

ENO photolysis: effect of initial pH

Previous studies usually report the bimolecular reaction rate constants between RPS and the neutral forms of the antibiotics (Boreen et al. 2004, 2005; Edhlund et al. 2006). Nevertheless, according to Ge et al. (2015), the $HO^•$ oxidation reactivity of the fluoroquinolones ciprofloxacin, danofloxacin, levofloxacin, sarafloxacin, difloxacin, and enrofloxacin would depend on their speciation at different pH values.

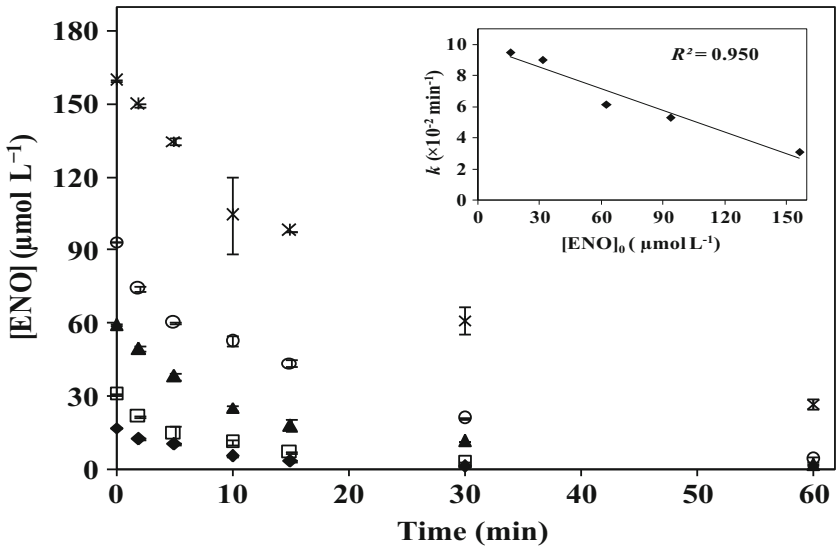

Fig. 1 ENO degradation under simulated solar radiation in Milli-Q water at pH 7 for different initial concentrations (in μmol L^{-1}): ♦ 15.6; □ 31.2; ▲ 62.4; ○ 93.7; * 156.1). Inset: effect of $[ENO]_0$ on the specific photolysis rates. Experiments run in duplicate

The results of ENO photolysis in Milli-Q water at pH 3, 7, and 9 indicated that degradation is more rapid at higher pH (Fig. 2). The pseudo first-order specific photolysis rates at pH 7 and 9 are $(9.0 \pm 0.63) \times 10^{-2}$ min^{-1} ($R^2 = 0.973$) and $(6.2 \pm 0.14) \times 10^{-2}$ min^{-1} ($R^2 = 0.995$), respectively (inset of Fig. 2). At pH 3, virtually no change in ENO concentration was observed after 60 min of irradiation. A longer experiment (4 h) was carried out in order to check ENO photolysis at pH 3, giving a pseudo first-order specific photolysis rate $k = (4.1 \pm 1.1) \times 10^{-4}$ min^{-1} ($R^2 = 0.975$), which is two orders of magnitude smaller in comparison with the values obtained at pH 7 and 9.

For ENO, the two equilibrium constants, $pK_{a1} = 6.0$ and $pK_{a1} = 8.5$, are attributed to the dissociation of a 3-carboxylic group and to the protonation of the 7-piperazinyl group (Sortino et al. 1998). It is worth observing that the cationic form of ENO is predominant under acidic conditions (pH < 6.0), the zwitterionic form predominates in the pH range 6.0–8.5, whereas the anionic form prevails at pH > 8.5 (Gao et al. 2011). The UV absorption spectrum of ENO at pH 7 (Fig. 3) shows two main bands centered at 264 and 345 nm; the corresponding molar absorption coefficients were 28,964 L mol and 17,491 L mol^{-1} cm^{-1}, respectively. Similar absorption behavior has been observed for other fluoroquinolones (Lorenzo et al. 2009).

Although light absorption is quite similar at different pH above 290 nm (from which the solar simulator effectively emits), the quantum yield for triplet formation and its lifetime have been shown to be high at neutral pH (Sortino et al. 1998). In fact, at pH 7, the ENO zwitterion predominates, and the quantum yield for the formation of the excited triplet state (^{3}ENO*) has been reported to be ≥ 0.5 (Albini and Monti 2003). Our results therefore agree with the reported photo-behavior of fluoroquinolones at different pH (Albini and Monti 2003; Porras et al. 2016). In fact, Porras et al. (2016) verified that the direct photolysis rates of ciprofloxacin (CIP) were low at pH 3, and noticeably enhanced at pH 7. The authors hypothesized that the rate of internal conversion from ^{1}CIP* to its electronic ground state is increased at low pH, which would decrease the formation efficiency of ^{3}CIP* from ^{1}CIP*.

From our experimental results, the ENO direct photolysis quantum yields (Φ_{ENO}) were calculated according to the approach of Schwarzenbach (2003), resulting $(1.08 \pm 0.28) \times 10^{-4}$, $(1.93 \pm 0.14) \times 10^{-2}$, and $(2.68 \pm 0.06) \times 10^{-2}$ mol ENO mol photons^{-1}, at pH 3, 7, and 9, respectively. The value at pH 7 is in very good agreement with the quantum yields of direct photolysis reported for six other FQs (ciprofloxacin, danofloxacin, levofloxacin, sarafloxacin, difloxacin, and enrofloxacin) under sunlight, ranging from 1.21×10^{-2} to 15.4×10^{-2} (Ge et al. (2015). Our experimental findings agree with the reported photo-behavior of fluoroquinolone antibiotics at different pH (Albini and Monti 2003; Porras et al. 2016). We therefore follow the reasoning of Porras et al. (2016), according to whom the rate of internal conversion from ^{1}ENO* to its electronic ground state would be increased at low pH, which would therefore decrease the formation efficiency of ^{3}ENO* from ^{1}ENO*, hence impacting its photolysis under acidic conditions. Moreover, it is worth remarking that the values of Φ_{ENO} we determined comprise different phenomena, i.e., direct photolysis and self-sensitized photo-oxidation via HO$^\bullet$ radicals and $^1O_2$, as previously discussed.

As pointed out by Parsons (2004), photolysis quantum yields may be affected by different factors: wavelength, pH, pollutant concentration, temperature, solvent, and dissolved oxygen concentration. In our study, the specific ENO photolysis rates and quantum yields were found to be highly pH-dependent as well. Other authors also observed pH-dependent photolysis quantum yields. For example, Maddigapu et al. (2011) obtained the UVA photolysis quantum yields of 2,4-

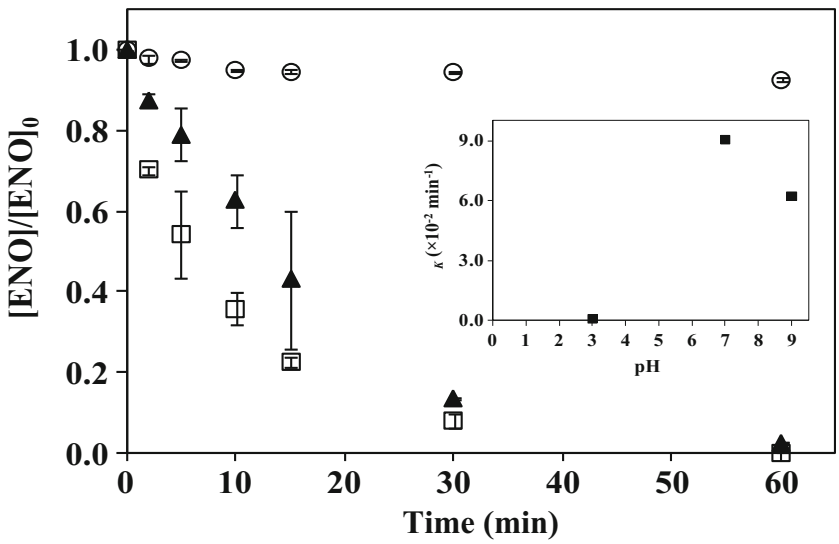

Fig. 2 ENO degradation under simulated solar radiation in Milli-Q water ($[ENO]_0 = 30.5 \pm 0.18$ μmol L^{-1}) for different pH: ○ 3; □ 7; ▲ 9. Inset: effect of pH on the specific photolysis rates. Experiments run in duplicate

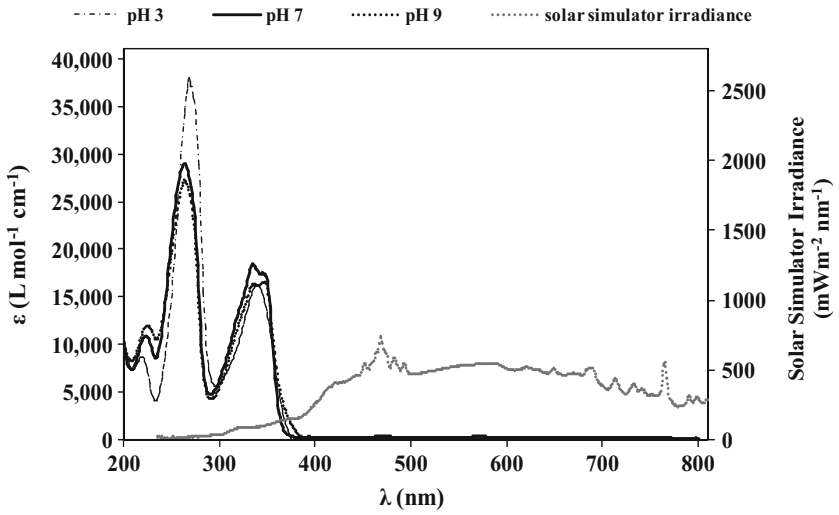

Fig. 3 Spectral decadic ENO molar absorption coefficients (ε) at different pH and emission spectrum of the solar simulator

dichloro-6-nitrophenol (DCNP) at pH 2.3 ($\Phi_{\text{undissociated DCNP}} = (2.75 \pm 0.46) \times 10^{-5}$) and pH 7.8 ($\Phi_{\text{phenolate}} = (4.53 \pm 0.78) \times 10^{-6}$). According to the authors, these results are consistent with a less efficient formation or a lower reactivity of the triplet state of the phenolate. Also, Boreen et al. (2005) measured the direct photolysis quantum yields for both the neutral and anionic species of five sulfa drugs containing six-membered heterocyclic substituents (sulfamethazine, sulfamerazine, sulfadiazine, sulfachloropyridazine, and sulfadimethoxine). The quantum yield values, which were also shown to be speciation dependent, ranged from 0.01×10^{-3} (neutral form of sulfadimethoxine) to 5×10^{-3} (anionic form of sulfamethazine). Similarly, the UV photolysis quantum yield of *N*-nitrosodimethylamine (NDMA) was also shown to be pH-dependent, with $\Phi_{\text{NDMA}} = 0.25$ at pH 3 and $\Phi_{\text{NDMA}} = 0.13$ at pH 7 (Stefan and Bolton 2002).

Figure 4 shows that Φ_{ENO} decreases with increasing $[\text{ENO}]_0$. The dependence of photolysis quantum yields with initial solute concentration has also been observed by other authors. Hessler et al. (1993) found the same trend for the atrazine and metazachlor UV (254 nm) photolysis quantum yields. In contrast, Bedini et al. (2012) studied the UVA photolysis of anthraquinone-2-sulfonate (AQ2S) in the concentration range 1 to 3 mmol L^{-1}, at pH 6. The values of Φ_{AQ2S} were shown to be independent of AQ2S concentration up to about 0.1 mmol L^{-1}, markedly increasing for higher $[\text{AQ2S}]_0$. These examples show that the quantum yield-concentration relationship apparently depends on the chemical nature of the solute being photolyzed.

Kinetic study of ENO degradation by reactive photo-induced species

The values of the second-order kinetic rate constants of ENO with reactive photo-induced species ($HO^{\bullet}$, $^1O_2$, ^{3}AQ2S*), obtained by the competition kinetics method in Milli-Q water

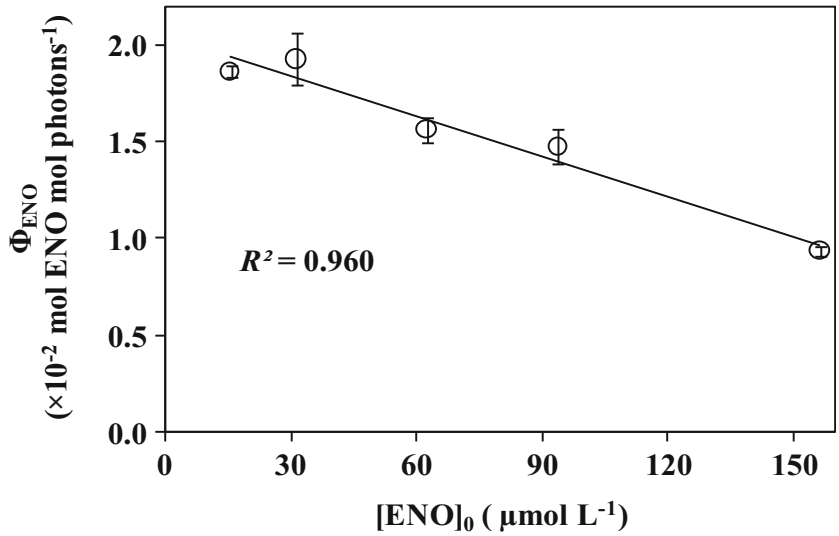

Fig. 4 Effect of $[\text{ENO}]_0$ on the photolysis quantum yields at pH 7. Experiments run in duplicate

at pH 3, 7, and 9, are listed in Table 1. The raw data and the corresponding kinetic treatment are provided in Online Resource 1-9.

The experimental values of $k_{ENO,HO\cdot}$ and $k_{ENO,3AQ2S*}$ are much higher than $k_{ENO,1O2}$, which indicates that hydroxyl radicals and ^{3}CDOM* should play a more important role in ENO degradation in comparison with singlet oxygen. Based on these results, the main pathways involved in ENO photodegradation in sunlit surface waters would be direct photolysis, the reaction with $HO^\bullet$, and the transformation induced by ^{3}CDOM*.

The *k*-pH relationship depicted in Table 1 can be attributed to different reactivities of protonated, zwitterionic, and anionic forms of ENO in aqueous solution. This effect is more noticeable for the electron transfer reaction (Barbieri et al. 2008) between the triplet excited states (^{3}AQ2S*) and electron-donor ENO molecules. In fact, the value of $k_{ENO,3AQ2S*}$ increased almost 30 times, when the initial pH changed from 3 to 7. Moreover, the results in Table 1 suggest that the zwitterionic form of ENO is the most reactive towards different reactive photo-induced species (RPS), which is in consonance with the literature regarding fluoroquinolones. As an example, for different fluoroquinolones (ciprofloxacin, danofloxacin, levofloxacin, sarafloxacin, difloxacin, and enrofloxacin), Ge et al. (2015) found that the neutral forms (HFQ^0) reacted faster with $HO^\bullet$ radicals, followed by the anionic (FQ^-) and protonated forms (H_2FQ^+). The effect of pH on the oxidation kinetics was attributed by the authors to different reactivities of individual protonated states of FQs towards hydroxyl radicals. In contrast, for hydroxylated polybrominated diphenyl ethers (HO-PBDEs), Xie et al. (2013) observed that the values of k_{1O2} and $k_{HO^\bullet}$ for the anions were much higher than those found for the neutral molecules. In conclusion, this behavior seems to depend strongly on the chemical nature of the target compound.

The values of $k_{ENO,1O2}$ in Table 1 are consistent with values previously reported for fluoroquinolones in aqueous solution (Albini and Monti 2003). For this class of antibiotics, the rate constants of singlet oxygen quenching reactions in aqueous medium lie in the range 10^6–10^7 L mol^{-1} s^{-1} and vary very little with FQ structure (Albini and Monti 2003). In the case of ^{3}AQ2S*, the values we obtained in this study are close to those determined for 2,4-dichloro-6-nitrophenol (DCNP) ($k_{DCNP,3CDOM*} = 1.36 \times 10^8$ L mol^{-1} s^{-1}) under UVA irradiation using the excited triplet state of anthraquinone-2-sulfonate as a proxy for ^{3}CDOM* (Maddigapu et al. 2011). The excited triplet states of CDOM are important reactive species in surface waters. However, the chemical composition of CDOM strongly depends on its origin; thus, it may be necessary to study the behavior of molecules that are representative of the composition and reactivity of CDOM, such as AQ2S. Therefore, comprehensive studies to determine the bimolecular reaction rate constants between antibiotics and ^{3}CDOM* are still lacking. As a final remark, Vione et al. (2011) studied the photochemical fate of ibuprofen in surface waters and used AQ2S and riboflavin (Ri) as CDOM proxies. The corresponding reaction rate constants between the target pharmaceutical and the triplet states at pH 8 were $k_{IBP,3AQ2S*} = (9.7 \pm 0.2) \times 10^9$ L mol^{-1} s^{-1} and $k_{IBP,3Ri*} = (4.5 \pm 0.4) \times 10^7$ L mol^{-1} s^{-1}. The later is two orders of magnitude lower at the same pH value, showing that the reactivity of organic pollutants with oxidant triplet excited states is greatly affected by the triplet nature.

Table 1 Second-order kinetic rate constants of ENO with reactive photo-induced species ($HO^\bullet$, $^1O_2$, ^{3}AQ2S*) in Milli-Q water at pH 3, 7, and 9. $[ENO]_0 = 31.8 \pm 2.41$ μmol L^{-1}

pH	$k_{ENO,1O2}$ ($\times 10^6$ L mol^{-1} s^{-1})	$k_{ENO,HO\cdot}$ ($\times 10^{10}$ L mol^{-1} s^{-1})	$k_{ENO,3AQ2S*}$ ($\times 10^8$ L mol^{-1} s^{-1})
3	2.5 ± 0.9	1.1 ± 0.3	2.7 ± 0.5
7	3.9 ± 0.2	14.0 ± 0.8	61.5 ± 0.7
9	1.7 ± 0.2	9.1 ± 1.0	6.5 ± 1.3

ENO photochemical degradation in the presence of dissolved organic matter

In general, organic matter may diminish pollutant removal by screening sunlight and scavenging reactive species or can improve contaminant photodegradation through the formation of $HO^\bullet$, $^1O_2$, and ^{3}DOM* (Guerard et al. 2009). Therefore, the overall effect of dissolved organic matter upon indirect photodegradation rates of organic pollutants depends on these two opposite effects (Carlos et al. 2012).

The chemical composition and photochemical properties of DOM depend on its source. Therefore, in order to study the indirect photolysis of ENO, experiments were carried out at pH 7 in the presence of Suwannee River natural organic matter SRNOM, urban-waste bio-organic substance (CVT230), and Aldrich humic acid sodium salt (AHA) at pH 7 (Fig. 5). CVT230 was isolated from urban residues (Montoneri et al. 2011), and in this study, it was used with the sake of comparison only.

The addition of CVT230 and SRNOM had a detrimental effect on ENO photodegradation (Fig. 5), which is also shown by the corresponding pseudo first-order specific degradation rates, varying from $(9.0 \pm 0.6) \times 10^{-2}$ min^{-1} ($R^2 = 0.973$) in the absence of DOM to $(4.9 \pm 0.6) \times 10^{-2}$ min^{-1} ($R^2 = 0.984$) and $(5.5 \pm 0.1) \times 10^{-2}$ min^{-1} ($R^2 = 0.978$) in the presence of SRNOM and CVT230, respectively. For these DOM, we hypothesize that screen and/or scavenging effects overcame the RPS-driven ENO degradation. In contrast, RPS formation upon irradiation of the Aldrich humic acid sodium salt (AHA) and their reaction with ENO probably played a more important role compared with screen and/or scavenging effects, in such

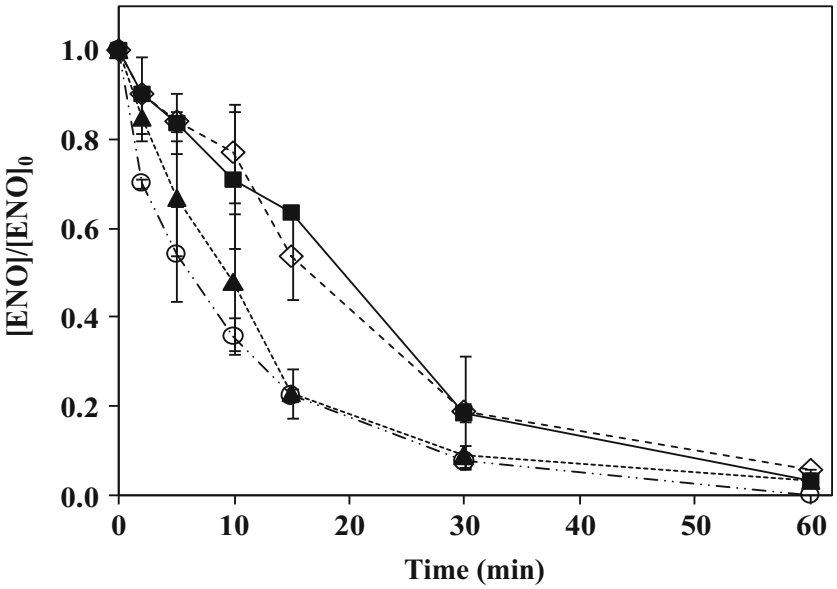

Fig. 5 Indirect photolysis of ENO ($[ENO]_0 = 30.6 \pm 1.96$ μmol L^{-1}) in Milli-Q water at pH 7 in the presence of 10 mg L^{-1} of different organic matter (▲ AHA; ■ CVT230; ◊ SRNOM; and ○ without DOM). Experiments run in duplicate

way that similar ENO concentration-time profiles were obtained in the presence or absence of the colored DOM. In addition, the corresponding pseudo first-order specific photolysis rates were higher: $(9.0 \pm 0.6) \times 10^{-2}$ min^{-1} (ENO) and $(6.4 \pm 0.3) \times 10^{-2}$ min^{-1} (ENO + AHA). It is worth remarking that ENO removal in the absence of DOM was quite fast, which is probably due to the self-sensitized photo-oxidation pathway proposed for fluoroquinolones (Li et al. 2014; Ge et al. 2015).

The humic substances (HS) constitute the main fraction of dissolved organic matter and can promote or retard the photochemical removal of organic contaminants under sunlight in aqueous systems. Carlos et al. (2012) studied the photochemical fate of a mixture of emerging pollutants in the presence of humic substances. The addition of HS resulted in an increase of indirect photoprocesses, with the main photodegradation pathway occurring by oxidation mediated by ^{3}HS*. On the other hand, Batista et al. (2016) studied the correlation between the chemical and spectroscopic characteristics of natural organic matter (NOM) with sulfamerazine photodegradation. The following NOM were used: SRNOM, Suwannee River humic acid (SRHA), Suwannee River fulvic acid (SRFA), and AHA. The later was found to be the most reactive towards sulfamerizine degradation. AHA is not representative of aquatic DOM but exhibited relatively high steady-state concentrations of ^{3}NOM*, high total fluorescence intensity, high $SUVA_{254}$, and aromatic content in comparison with the other DOM investigated (Batista et al. 2016).

Photochemical modeling

Figure 6 presents the predicted ENO half-life times ($t_{1/2}$) as a function of water depth, DOC, $[NO_2^-]$, and $[HCO_3^-]$ under summertime irradiation conditions. According to the APEX simulations, the $t_{1/2}$ values vary from a few hours to days.

As observed in Fig. 6a, the antibiotic is degraded faster in shallow water bodies and/or at low DOC levels. The ENO half-life increases from 7 h to 1.3 days (0.5-m water depth) and from 13 h to 5 days (5-m water depth) when the dissolved organic carbon (DOC) increases from 0.5 to 10 mg L^{-1}. Additionally, for a 10-fold increase in depth, $t_{1/2}$ increases 81 and 318% for the minimum and maximum DOC levels, respectively. Similar results were obtained by Fabbri et al. (2015) who studied the photochemical fate of cephalosporins in surface waters and reported amoxicillin half-life times increasing up to a plateau with increasing DOC (Fabbri et al. 2015). According to Passananti et al. (2014), high DOC means elevated DOM and CDOM contents. For high DOC, direct photolysis can be affected due to the competitive effect between the substrate and CDOM for sunlight photons. In addition, while CDOM is a photochemical source of $HO^\bullet$ radicals, DOM can act as an important $HO^\bullet$ scavenger (Fabbri et al. 2015).

Figure 6b shows the ENO half-life time as a function of nitrite and DOC concentrations, for 2.75-m water depth. Due to the importance of the reaction with $HO^\bullet$ radicals, the photochemical fate of organic pollutants in surface waters increases slightly for higher nitrate and nitrite concentrations. In this case, a 300-fold increase in nitrite concentration contributes to a 1.9- and 1.2-fold decrease in $t_{1/2}$ at low and high DOC levels, respectively. As expected, ENO degradation becomes notably slower with increasing DOC concentration. The ENO half-life time increased from 17.9 h to 3.9 days (low $[NO_2^-] = 5 \times 10^{-2}$ μmol L^{-1}) and from 9.3 h to 3.2 days (high $[NO_2^-] = 15$ μmol L^{-1}) when dissolved organic carbon (DOC) increases from 0.5 to 10 mg L^{-1}. Therefore, the model simulations indicate that enoxacin is degraded faster at low DOC levels, as expected, and the impact of nitrite anions upon the antibiotic persistence is small. Silva et al. (2015) studied the photochemical fate of the herbicide amicarbazone. For the

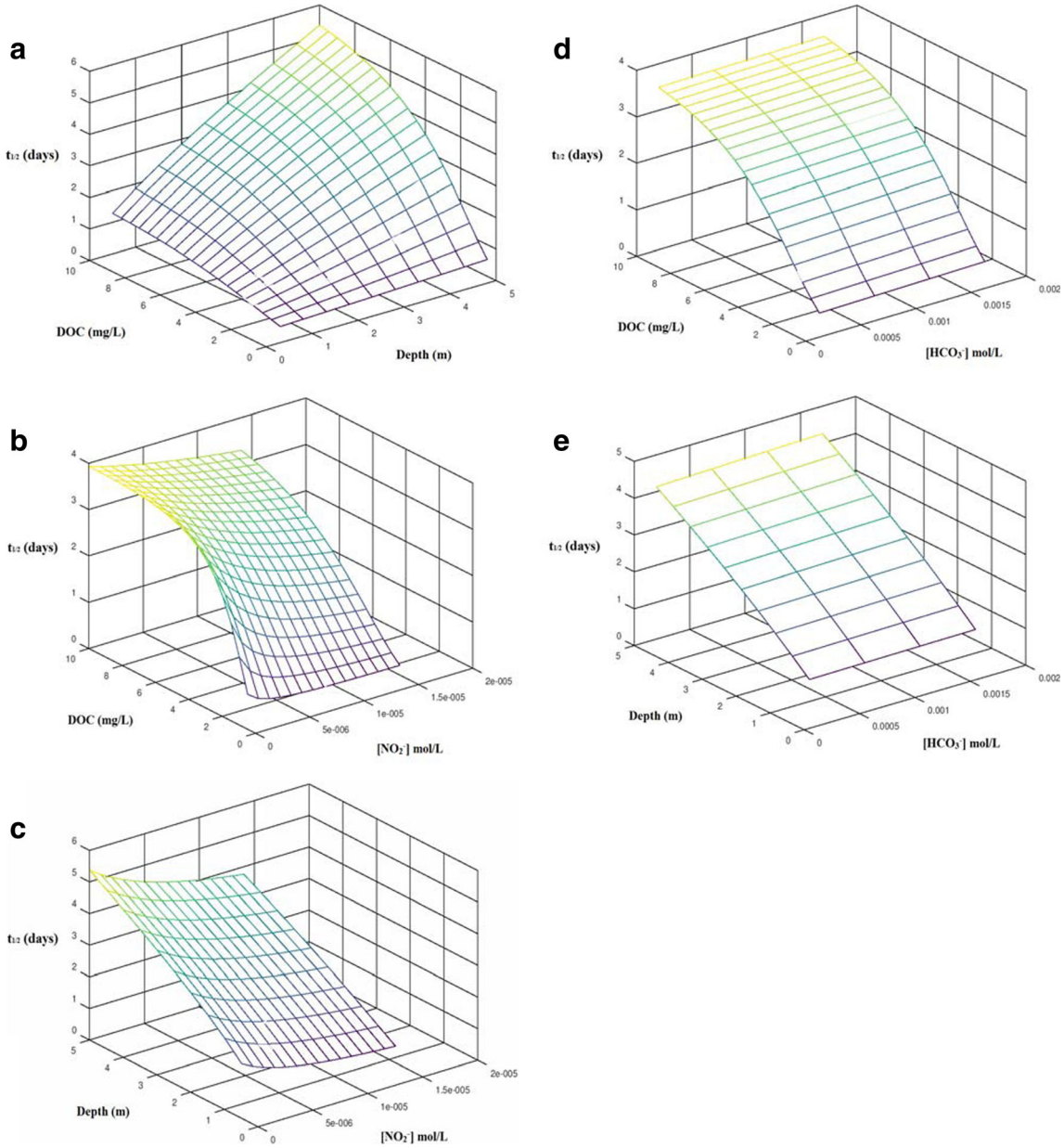

Fig. 6 Results of the simulations using the APEX model regarding the effect of different variables (water depth, DOC, $[NO_2^-]$, and $[HCO_3^-]$) on ENO half-life time ($t_{1/2}$) under summertime irradiation at pH 7

same increase in $[NO_2^-]$, the APEX simulations indicated a slight decrease in amicarbazone half-life at higher DOC concentrations. In contrast, an increase in nitrite concentration at low DOC levels contributed to a 3-fold increase in $t_{1/2}$. The authors explain that the impact of nitrite anions on the herbicide degradation depends on the composition of the key role species (DOC, HCO_3^-, and CO_3^{2-}) in natural aqueous systems.

In Fig. 6c, a pronounced influence of water depth on ENO persistence in natural systems is clearly seen. For a 10-fold increase in depth, 3-fold and almost 5-fold increases in $t_{1/2}$ values are observed for the minimum and maximum NO_2^- concentration levels, respectively. In contrast, for a 300-fold increase in $[NO_2^-]$, the half-life decreases 55 and 30% for the minimum and maximum depth levels, respectively. Silva et al. (2015) explained that the combined effect of nitrite and water depth on amicarbazone half-life does not depend on nitrate and bicarbonate levels. Similar results were obtained by Fabbri et al. (2015), who reported that water parameters such as nitrate, nitrite, and inorganic carbon would be barely important for amoxicillin direct photolysis.

Figure 6d, e shows the ENO half-life time as a function of bicarbonate and DOC concentrations or water depth. For a 10-fold increase in HCO_3^- concentration, $t_{1/2}$ increases only 18 and 2% for the minimum and maximum DOC levels, respectively. In contrast with the effect of HCO_3^-, for a 20-fold

increase in DOC concentration, 9-fold and 8-fold increases in half-life are observed for the minimum and maximum HCO_3^- levels, respectively. As pointed out by Silva et al. (2015), these tendencies show a much more pronounced scavenging of hydroxyl radicals by DOM in comparison with bicarbonate/carbonate anions in natural aqueous systems.

Reactions with ^{3}CDOM* can be important ENO transformation pathways in sunlit surface waters. In fact, mathematical simulations using the experimental value of $k_{ENO,3AQ2S*}$ (under the hypothesis that $k_{ENO,3CDOM*} \sim k_{ENO,3AQ2S*}$) showed that ENO half-life increases from 5.4 to 13 days, for the maximum depth (5 m) and DOC (10 mg L^{-1}) levels. Such a scenario is compatible with previous studies carried out with ibuprofen, suggesting that $HO^\bullet$ radical-mediated reactions would not be the only relevant transformation pathway in surface waters (Vione et al. 2011). In this case, Vione et al. (2011) showed that, for high DOC levels, the most relevant ibuprofen degradation pathways in surface water are, in the order of importance, $HO^\bullet$ attack, direct photolysis, and reactions with ^{3}CDOM*.

Conclusions

ENO photodegradation follows apparent first-order behavior, with specific photolysis rates and percent removals higher at neutral pH, and decreasing with increasing antibiotic initial concentration. The zwitterionic form of ENO, which prevails at the typical pH values of surface waters, shows second-order reaction rate constants of $(14.0 \pm 0.8) \times 10^{10}$, $(3.9 \pm 0.2) \times 10^6$, and $(61.5 \pm 0.7) \times 10^8$ L mol^{-1} s^{-1} with $HO^\bullet$, $^1O_2$, and ^{3}AQ2S* (selected as CDOM proxy), respectively. The differences observed for these k values at pH 3, 7, and 9 can be attributed to changes in ENO photochemical reactivity related to its pH-dependent speciation. The prevailing pathways involved in the sunlight-driven enoxacin degradation in water are its direct photolysis and the reactions with $HO^\bullet$ and ^{3}AQ2S*.

The mathematical simulations indicate that the electron transfer reaction with ^{3}CDOM* can be an important ENO transformation pathways in surface waters exposed to sunlight. DOM and water depth are expected to have the highest impacts on ENO half-life time, varying from a few hours to days during summertime, depending on the concentrations of waterborne, environmentally-relevant species (organic matter, NO_3^-, NO_2^-, HCO_3^-).

The persistence of antibiotics in sunlit surface waters, even in small concentrations, may lead to the emergence of bacterial resistance, with possible impacts on the aquatic biota and human health. The results of the present study suggest that suitable advanced oxidation treatment processes are recommended for the remediation of ENO-containing wastewaters in order to prevent this emerging contaminant from entering aqueous environments.

Acknowledgements The authors express their gratitude to FAPESP (São Paulo Research Foundation, grant #2016/03695-8) and to Prof. Neyde Y. M. Iha (Laboratory of Photochemistry and Energy Conversion of the Institute of Chemistry, University of São Paulo, Brazil).

References

al Housari F, Vione D, Chiron S, Barbati S (2010) Reactive photoinduced species in estuarine waters. Characterization of hydroxyl radical, singlet oxygen and dissolved organic matter triplet state in natural oxidation processes. Photochem Photobiol Sci 9:78–86

Albini A, Monti S (2003) Photophysics and photochemistry of fluoroquinolones. Chem Soc Rev 32:238–250

Arques A, Bianco Prevot A (2015) Soluble bio-based substances isolated from urban wastes: environmental applications. Springer International Publishing, ISBN 978-3-31914744-4 (eBook), https://doi.org/10.1007/978-3-319-14744-4

Barbieri Y, Massad WA, Diaz DJ, Sanz J, Amat-Guerri F, Garcia NA (2008) Photodegradation of bisphenol a and related compounds under natural-like conditions in the presence of riboflavin: kinetics, mechanism and photoproducts. Chemosphere 73:564–571

Batista APS, Teixeira A, Cooper WJ, Cottrell BA (2016) Correlating the chemical and spectroscopic characteristics of natural organic matter with the photodegradation of sulfamerazine. Water Res 93:20–29

Bedini A, De Laurentiis E, Sur B, Maurino V, Minero C, Brigante M, Mailhot G, Vione D (2012) Phototransformation of anthraquinone-2-sulphonate in aqueous solution. Photochem Photobiol Sci 11:1445–1453

Bodrato M, Vione D (2014) APEX (aqueous photochemistry of environmentally occurring Xenobiotics): a free software tool to predict the kinetics of photochemical processes in surface waters. Environ Sci-Proc Imp 16:732–740

Boreen AL, Arnold WA, McNeill K (2004) Photochemical fate of sulfa drugs in the aquatic environment: sulfa drugs containing five-membered heterocyclic groups. Environ Sci Technol 38:3933–3940

Boreen AL, Arnold WA, McNeill K (2005) Triplet-sensitized photodegradation of sulfa drugs containing six-membered heterocyclic groups: identification of an SO_2 extrusion photoproduct. Environ Sci Technol 39:3630–3638

Carlos L, Martire DO, Gonzalez MC, Gomis J, Bernabeu A, Amat AM, Arques A (2012) Photochemical fate of a mixture of emerging pollutants in the presence of humic substances. Water Res 46:4732–4740

De Laurentiis E, Prasse C, Ternes TA, Minella M, Maurino V, Minero C, Sarakha M, Brigante M, Vione D (2014) Assessing the photochemical transformation pathways of acetaminophen relevant to surface waters: transformation kinetics, intermediates, and modelling. Water Res 53:235–248

Edhlund BL, Arnold WA, McNeill K (2006) Aquatic photochemistry of nitrofuran antibiotics. Environ Sci Technol 40:5422–5427

Elovitz MS, von Gunten U (1999) Hydroxyl radical ozone ratios during ozonation processes. I-the R-ct concept. Ozone-Sci Eng 21:239–260

Escalada JP, Arce VB, Porcal GV, Biasutti MA, Criado S, Garcia NA, Martire DO (2014) The effect of dichlorophen binding to silica nanoparticles on its photosensitized degradation in water. Water Res 50:229–236

Fabbri D, Minella M, Maurino V, Minero C, Vione D (2015) A model assessment of the importance of direct photolysis in the photo-fate of cephalosporins in surface waters: possible formation of toxic intermediates. Chemosphere 134:452–458

Fick J, Soderstrom H, Lindberg RH, Phan C, Tysklind M, Larsson DGJ (2009) Contamination of surface, ground, and drinking water from pharmaceutical production. Environ Toxicol Chem 28:2522–2527

Gangwang, Liu GG, Liu HJ, Zhang N, Wang YL (2012) Photodegradation of salicylic acid in aquatic environment: effect of different forms of nitrogen. Sci Total Environ 435:573–577

Gao SQ, Jin HY, You JY, Ding Y, Zhang N, Wang Y, Ren RB, Zhang R, Zhang HQ (2011) Ionic liquid-based homogeneous liquid-liquid microextraction for the determination of antibiotics in milk by high-performance liquid chromatography. J Chromatogr A 1218: 7254–7263

Ge LK, Na GS, Zhang SY, Li K, Zhang P, Ren HL, Yao ZW (2015) New insights into the aquatic photochemistry of fluoroquinolone antibiotics: direct photodegradation, hydroxyl-radical oxidation, and antibacterial activity changes. Sci Total Environ 527:12–17

Guerard JJ, Miller PL, Trouts TD, Chin YP (2009) The role of fulvic acid composition in the photosensitized degradation of aquatic contaminants. Aquat Sci 71:160–169

Hessler DP, Gorenflo V, Frimmel FH (1993) Degradation of aqueous atrazine and Metazachlor solutions by UV and UV/H_2O_2 - influence of pH and herbicide concentration. Acta Hydrochirn Hydrobiol 21: 209–214

Ji YF, Zhou L, Zhang Y, Ferronato C, Brigante M, Mailhot G, Yang X, Chovelon JM (2013) Photochemical degradation of sunscreen agent 2-phenylbenzimidazole-5-sulfonic acid in different water matrices. Water Res 47:5865–5875

Larsson DGJ, de Pedro C, Paxeus N (2007) Effluent from drug manufactures contains extremely high levels of pharmaceuticals. J Hazard Mater 148:751–755

Li K, Zhang P, Ge LK, Ren HL, Yu CY, Chen XY, Zhao YF (2014) Concentration-dependent photodegradation kinetics and hydroxyl-radical oxidation of phenicol antibiotics. Chemosphere 111:278–282

Liu YM, Shi YM, Liu ZL (2010) Determination of enoxacin and ofloxacin by capillary electrophoresis with electrochemiluminescence detection in biofluids and drugs and its application to pharmacokinetics. Biomed Chromatogr 24:941–947

Lorenzo F, Navaratnam S, Edge R, Allen NS (2009) Primary Photoprocesses in a Fluoroquinolone antibiotic Sarafloxacin. Photochem Photobiol 85:886–894

Maddigapu PR, Minella M, Vione D, Maurino V, Minero C (2011) Modeling Phototransformation reactions in surface water bodies: 2,4-Dichloro-6-Nitrophenol as a case study. Environ Sci Technol 45:209–214

Marchetti G, Minella M, Maurino V, Minero C, Vione D (2013) Photochemical transformation of atrazine and formation of photointermediates under conditions relevant to sunlit surface waters: laboratory measures and modelling. Water Res 47:6211–6222

Montoneri E, Boffa V, Savarino P, Perrone D, Ghezzo M, Montoneri C, Mendichi R (2011) Acid soluble bio-organic substances isolated from urban bio-waste. Chemical composition and properties of products. Waste Manag 31:10–17

Mostafa S, Rosario-Ortiz FL (2013) Singlet oxygen formation from wastewater organic matter. Environ Sci Technol 47:8179–8186

Parsons S (2004) Advanced oxidation processes for water and wastewater treatment. IWA Publishing, London

Passananti M, Temussi F, Iesce MR, Previtera L, Mailhot G, Vione D, Brigante M (2014) Photoenhanced transformation of nicotine in aquatic environments: involvement of naturally occurring radical sources. Water Res 55:106–114

Perisa M, Babic S, Skoric I, Fromel T, Knepper TP (2013) Photodegradation of sulfonamides and their N (4)-acetylated metabolites in water by simulated sunlight irradiation: kinetics and identification of photoproducts. Environ Sci Pollut R 20:8934–8946

Porras J, Bedoya C, Silva-Agredo J, Santamaria A, Fernandez JJ, Torres-Palma RA (2016) Role of humic substances in the degradation pathways and residual antibacterial activity during the photodecomposition of the antibiotic ciprofloxacin in water. Water Res 94:1–9

Schwarzenbach RP (2003) Environmental organic chemistry. Second edition. Wiley & Sons, Inc., Hoboken

Silva MP, Mostafa S, McKay G, Rosario-Ortiz FL, Teixeira A (2015) Photochemical fate of Amicarbazone in aqueous media: laboratory measurement and simulations. Environ Eng Sci 32:730–740

Sortino S, De Guidi G, Giuffrida S, Monti S, Velardita A (1998) pH effects on the spectroscopic and photochemical behavior of Enoxacin: a steady-state and time-resolved study. Photochem Photobiol 67:167–173

Stefan MI, Bolton JR (2002) UV direct photolysis of *N*-Nitrosodimethylamine (NDMA): kinetic and product study. Helv Chim Acta 85:1416–1426

Tong CL, Xiang GH (2007) Sensitive determination of enoxacin by its enhancement effect on the fluorescence of terbium(III)-sodium dodecylbenzene sulfonate and its luminescence mechanism. J Lumin 126:575–580

Vione D, Maddigapu PR, De Laurentiis E, Minella M, Pazzi M, Maurino V, Minero C, Kouras S, Richard C (2011) Modelling the photochemical fate of ibuprofen in surface waters. Water Res 45:6725–6736

Xie Q, Chen J, Zhao H, Qiao X, Cai X, Li X (2013) Different photolysis kinetics and photooxidation reactivities of neutral and anionic hydroxylated polybrominated diphenyl ethers. Chemosphere 90: 188–194